Granular cooling of hard needles

Martin Huthmann, Timo Aspelmeier, and Annette Zippelius

Institut für Theoretische Physik, Universität Göttingen, D-37073 Göttingen, Germany

(Received 9 February 1999)

We have developed a kinetic theory of hard needles undergoing binary collisions with loss of energy due to normal and tangential restitution. In addition, we have simulated many particle systems of granular hard needles. The theory, based on the assumption of a homogeneous cooling state, predicts that granular cooling of the needles proceeds in two stages: An exponential decay of the initial configuration to a state where translational and rotational energies take on a time independent ratio (different from unity), followed by an algebraic decay of the total kinetic energy $\sim t^{-2}$. The simulations support the theory very well for low and moderate densities. For higher densities, we have observed the onset of the formation of clusters and shear bands. [S1063-651X(99)00407-9]

I. INTRODUCTION

Gas kinetics of inelastically colliding particles has received a lot of interest in recent years, mainly in the context of granular matter [1]. Boltzmann's equation has been generalized to inelastic collisions which are characterized by normal restitution and possibly tangential friction or restitution [2]. Extensive simulations have been performed, in particular event driven (ED) algorithms are very effective for the kinetic gas regime. A variety of interesting phenomena have been observed, for example instabilities of the homogeneous state towards shearing or clustering [3–5]. Most studies so far have concentrated on spherically symmetric objects, whereas real grains are in general nonspherical and often randomly shaped. The question arises whether the observed phenomena are generic for granular matter or specific for spherical objects.

In this paper we discuss the cooling properties of hard needles in terms of a time evolution operator, which accounts for the exchange of translational and rotational energy as well as for normal and tangential restitution. In addition we have performed ED simulations of large systems with up to 20 000 needles.

For low and moderate densities the system does not show any clustering instabilities but remains homogeneous on the longest time scales, when the energy has decayed to 10^{-11} of its initial value. This allows us to formulate an approximate kinetic theory, based on the assumption of a homogeneous state. Cooling is found to proceed in two stages: (1) A fast exponential decay to a state which is characterized by a time independent ratio c of translational to rotational energy. (2) A slow algebraic decay like t^{-2} of the total kinetic energy. The latter is determined by the coefficient of restitution and by the distribution of mass along the needles, including equipartition for one particular mass distribution. Simulations and approximate analytical theory are found to agree within a few percent.

For high densities we observe long range correlations in the velocity field and a buildup of large density fluctuations. These large-scale structures are similar to those seen in dense systems of smooth spheres [3–6]. No alignment of the needles with the hydrodynamic flow field is observed.

II. DYNAMICS OF COLLISIONS

Consider two rods of equal length L, mass m and moment of inertia I. The center of mass coordinates are denoted by r_1 and r_2. The orientations are specified by unit vectors u_1 and u_2, which span a plane E_{12} with normal

$$u_\perp = \frac{u_1 \times u_2}{|u_1 \times u_2|}. \tag{1}$$

We decompose $r_{12} = r_1 - r_2$ into a component perpendicular $r_{12}^\perp = (r_{12} \cdot u_\perp) u_\perp$ and parallel $r_{12}^\parallel =: (s_{12} u_1 - s_{21} u_2)$ to E_{12} (see Fig. 1). The rods are in contact [7,8] if $r_{12}^\perp = 0$ and simultaneously $|s_{12}| < L/2$ and $|s_{21}| < L/2$.

We want to determine the postcollisional center-of-mass velocities (v_1', v_2') and angular velocities (ω_1', ω_2') in terms of the precollisional velocities $(v_1, v_2, \omega_1, \text{ and } \omega_2)$ or momenta $(p_1 = m v_1, p_2 = m v_2)$. Conservation of total linear momentum implies

$$p_1' = p_1 + \Delta p,$$
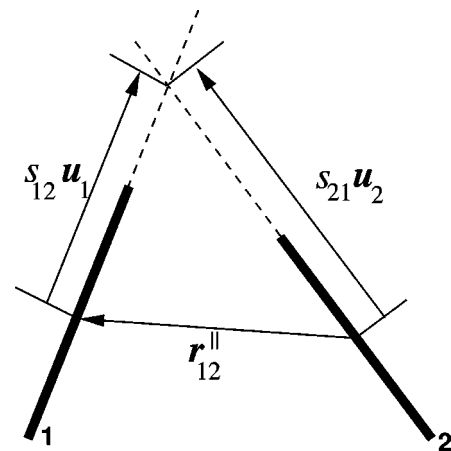
$$p_2' = p_2 - \Delta p. \tag{2}$$

FIG. 1. Configuration of two needles projected in the plane E_{12} spanned by the unit vectors u_1 and u_2.

PRE <u>60</u>   654

No torque acts at the points of contact, so that

$$\boldsymbol{\omega}_1' = \boldsymbol{\omega}_1 + \frac{s_{12}}{I}\boldsymbol{u}_1 \times \Delta\boldsymbol{p}, \quad \boldsymbol{\omega}_2' = \boldsymbol{\omega}_2 - \frac{s_{21}}{I}\boldsymbol{u}_2 \times \Delta\boldsymbol{p} \quad (3)$$

holds. To determine the collision process we consider the relative velocity of the contact points which is given by

$$\boldsymbol{V}_r = \frac{\boldsymbol{p}_1 - \boldsymbol{p}_2}{m} + s_{12}\dot{\boldsymbol{u}}_1 - s_{21}\dot{\boldsymbol{u}}_2. \quad (4)$$

We introduce two parameters ϵ and β to characterize normal and tangential restitution:

$$\boldsymbol{V}_r' \cdot \boldsymbol{u}_\perp = -\epsilon \boldsymbol{V}_r \cdot \boldsymbol{u}_\perp, \quad \epsilon \in [0,1], \quad (5)$$

$$\boldsymbol{V}_r' \cdot \boldsymbol{u}_1 = -\beta \boldsymbol{V}_r \cdot \boldsymbol{u}_1, \quad (6)$$

$$\boldsymbol{V}_r' \cdot \boldsymbol{u}_2 = -\beta \boldsymbol{V}_r \cdot \boldsymbol{u}_2, \quad \beta \in [-1,1]. \quad (7)$$

The above equations characterize the collision process completely and determine the postcollisional momenta in terms of the precollisional ones.

In this paper we specialize to the case of perfectly smooth needles, i.e., $\beta = -1$, which considerably simplifies the collision rules. The change of linear momentum is then given by $\Delta\boldsymbol{p} = \alpha\boldsymbol{u}_\perp$ with

$$\alpha = \frac{-(1+\epsilon)(\boldsymbol{V}_r \cdot \boldsymbol{u}_\perp)}{2/m + (s_{12}^2 + s_{21}^2)/I}. \quad (8)$$

III. ANALYTICAL THEORY

The derivation of a pseudo-Liouville operator for a system of N colliding, hard rods proceeds similar to the case of hard spheres [6,9,10]. The rods are confined to a three-dimensional volume V and interact via a hard core potential. The velocity of orientation $\dot{\boldsymbol{u}}_1 = \boldsymbol{\omega}_1 \times \boldsymbol{u}_1$ is confined to the plane perpendicular to $\boldsymbol{u}_1$ and is therefore described by *two* generalized canonical momenta, $p_{\theta_1} = I\dot{\theta}_1$ and $p_{\phi_1} = I\dot{\phi}_1 \sin^2\theta_1$, using spherical coordinates for the orientation. The total kinetic energy then reads

$$\mathcal{H}_{\text{kin}} = \sum_{i=1}^{N} \left(\frac{1}{2M}\boldsymbol{p}_i^2 + \frac{1}{2I}p_{\theta_i}^2 + \frac{1}{2I\sin^2\theta_i}p_{\phi_i}^2 \right). \quad (9)$$

The time development of a dynamical variable $A = A(\{\boldsymbol{r}_i(t), \boldsymbol{u}_i(t), \boldsymbol{p}_i(t), \dot{\boldsymbol{u}}_i(t)\})$ for positive times is determined by the pseudo-Liouville operator $\mathcal{L}_+$

$$A(\{\boldsymbol{r}_i, \boldsymbol{u}_i, \boldsymbol{p}_i, \dot{\boldsymbol{u}}_i\}, t) = \exp(i\mathcal{L}_+ t)A(\{\boldsymbol{r}_i, \boldsymbol{u}_i, \boldsymbol{p}_i, \dot{\boldsymbol{u}}_i\}, 0). \quad (10)$$

The pseudo-Liouville operator consists of two parts, $\mathcal{L}_+ = \mathcal{L}_0 + \mathcal{L}_+'$. The first describes free streaming and can be expressed by the Poisson bracket with the kinetic part of the Hamiltonian $i\mathcal{L}_0 = \{\mathcal{H}_{\text{kin}}, \dots\}_{\text{P.B.}}$. The second, $\mathcal{L}_+'$, describes binary collisions of two hard rods

$$i\mathcal{L}_+' = \frac{1}{2}\sum_{i\neq j}\left|\frac{d}{dt}|\boldsymbol{r}_{ij}^\perp|\right|\Theta\left(-\frac{d}{dt}|\boldsymbol{r}_{ij}^\perp|\right)\Theta(L/2 - |s_{ij}|)$$
$$\times \Theta(L/2 - |s_{ji}|)\delta(|\boldsymbol{r}_{ij}^\perp| - 0^+)(b_{ij} - 1). \quad (11)$$

Here $\Theta(x)$ is the Heaviside step function. The interpretation of the pseudo-Liouville operator of Eq. (11) is intuitively clear. The factor $|d/dt|\boldsymbol{r}_{ij}^\perp||$ is the component of the relative velocity of the contact points perpendicular to both rods. It yields the flux of incoming particles. $\Theta(-d/dt|\boldsymbol{r}_{ij}^\perp|)$ is nonzero only if the two particles are approaching and $\Theta(L/2 - |s_{ij}|)\Theta(L/2 - |s_{ji}|)\delta(|\boldsymbol{r}_{ij}^\perp| - 0^+)$ specifies the conditions for a collision to take place. The operator b_{ij} replaces momenta and angular momenta of particles i and j before collision by the corresponding ones after collision.

The time evolution of nonequilibrium expectation values of an observable $A(\{\boldsymbol{r}_i, \boldsymbol{u}_i, \boldsymbol{p}_i, \dot{\boldsymbol{u}}_i\}, t) = A(\Gamma; t)$ is defined by

$$\langle A \rangle_t = \int d\Gamma\rho(\Gamma; 0)A(\Gamma; t) = \int d\Gamma\rho(\Gamma; t)A(\Gamma; 0). \quad (12)$$

Γ denotes the whole phase space and $\rho(\Gamma; t)$ is the N-particle phase space distribution function, whose time evolution $\rho(\Gamma; t) = \exp(-i\mathcal{L}_+^\dagger t)\rho(\Gamma; 0)$ is governed by the adjoint $\mathcal{L}_+^\dagger$ of the time evolution operator $\mathcal{L}_+$. Here we are interested in the average translational and rotational kinetic energy per particle $E_{\text{tr}} = m/(2N)\Sigma_i\boldsymbol{v}_i^2$ and $E_{\text{rot}} = I/(2N)\Sigma_i\boldsymbol{\omega}_i^2$, as well as the total kinetic energy $E = E_{\text{tr}} + E_{\text{rot}}$.

It is impossible to calculate expectation values as given in Eq. (12) exactly and we are forced to approximate the N-particle distribution function. We assume that the system stays spatially homogeneous and that both linear and angular momenta are normally distributed. In a system which is prepared in a thermal equilibrium state the initial decay rates can be computed exactly and yield different values for averaged translational and rotational energy. This suggests defining two different temperatures for the translational and rotational degrees of freedom, corresponding to the following ansatz for the N particle distribution function [10]:

$$\rho_{\text{HCS}}(\Gamma; t) \sim \exp\left[-\frac{E_{\text{tr}}}{T_{\text{tr}}(t)} - \frac{E_{\text{rot}}}{T_{\text{rot}}(t)}\right]. \quad (13)$$

$\rho_{\text{HCS}}(\Gamma; t)$ depends on time via the average translational $T_{\text{tr}}(t) = 2/3\langle E_{\text{tr}}\rangle$ and rotational energy $T_{\text{rot}}(t) = \langle E_{\text{rot}}\rangle$. We are interested in the cooling properties of a gas of hard needles and compute the expectation values $\dot{T}_{\text{tr}} = 2/3\langle i\mathcal{L}_+E_{\text{tr}}\rangle$ and $\dot{T}_{\text{rot}} = \langle i\mathcal{L}_+E_{\text{rot}}\rangle$. Using the approximate many particle distribution of Eq. (13), we find two coupled differential equations

$$\frac{2\dot{T}_{\text{tr}}}{\gamma T_{\text{tr}}^{3/2}(1+\epsilon)} = -\int_\square d^2r \frac{\left(1 + \dfrac{T_{\text{rot}}}{T_{\text{tr}}}kr^2\right)^{1/2}}{1+kr^2}$$
$$+ \frac{1+\epsilon}{2}\int_\square d^2r \frac{\left(1 + \dfrac{T_{\text{rot}}}{T_{\text{tr}}}kr^2\right)^{3/2}}{(1+kr^2)^2}, \quad (14)$$

$$\frac{4\dot{T}_{\rm rot}}{3\gamma T_{\rm tr}^{3/2}(1+\epsilon)} = -\int_{\square} d^2r \frac{\dfrac{T_{\rm rot}}{T_{\rm tr}}kr^2\left(1+\dfrac{T_{\rm rot}}{T_{\rm tr}}kr^2\right)^{1/2}}{1+kr^2}$$

$$+\frac{1+\epsilon}{2}\int_{\square} d^2r \frac{kr^2\left(1+\dfrac{T_{\rm rot}}{T_{\rm tr}}kr^2\right)^{3/2}}{(1+kr^2)^2},$$

$$(15)$$

with $\gamma=(2NL^2\sqrt{\pi})/(3V\sqrt{m})$ and $k=(mL^2)/(2I)$. The two dimensional integration extends over a square of unit length, centered at the origin.

IV. SIMULATIONS

Simulations are performed using an event driven algorithm where the particles follow an undisturbed translational and rotational motion until a collision occurs. The velocities after the collision are computed according to the collision rules Eqs. (2)–(8). For this algorithm collision times for each pair of needles have to be determined numerically, where we follow the algorithm proposed by Frenkel and Maguire [7]. More efficiency is achieved by using the stratagem of Lubachevsky [11] and a linked cell structure, which allows us to look for collision partners only in the neighborhood. The algorithm is reasonably fast as long as there are only few needles in each cell of the linked cell structure, so that the time consuming search for collisions is restricted to the few needles in their own and the neighboring cells. On the other hand, we have to choose the linear dimension of these cells to be larger than the length of a needle, so that for high densities there are many needles in each cell and the algorithm becomes slow.

We mention here that the algorithm runs into numerical problems if the time between two collisions becomes too short to be resolved properly as it usually happens during an inelastic collapse. To circumvent this problem, we use the t_c model [12]: if the time between a collision and the preceding one for at least one particle is smaller than a critical value t_c, ϵ is set to 1. We believe that the influence of this procedure is small: there occurred only two instances in the simulations presented here.

We performed large scale simulations for various values of ϵ in the regime of small and moderate densities $[(N/V)L^3\lesssim 1]$. For high densities $[(N/V)L^3\gtrsim 10]$ only a few simulations could be done. We show here a simulation of $N=20\,000$ needles in a box of length $12L$ with $\epsilon=0.9$.

V. HYDRODYNAMIC QUANTITIES

To investigate deviations from *homogeneity*, we divide the simulation box into cells whose linear dimension is chosen to be large compared to the length of the needles but small compared to the box size. Given the limitations due to finite size we choose cells such that on average about 25 needles are in one cell. We then compute for each cell the number density $\rho_\alpha=(1/V_{\rm cell})\Sigma_{i\in{\rm cell}_\alpha}1=:\langle 1\rangle_\alpha$, the translational energy per particle $\rho_\alpha E_\alpha^{\rm tr}=\langle(m/2)\boldsymbol{v}_i^2\rangle_\alpha$ and the hydrodynamic temperature $T_\alpha^{\rm tr}=E_\alpha^{\rm tr}-m\boldsymbol{U}_\alpha^2/2$.
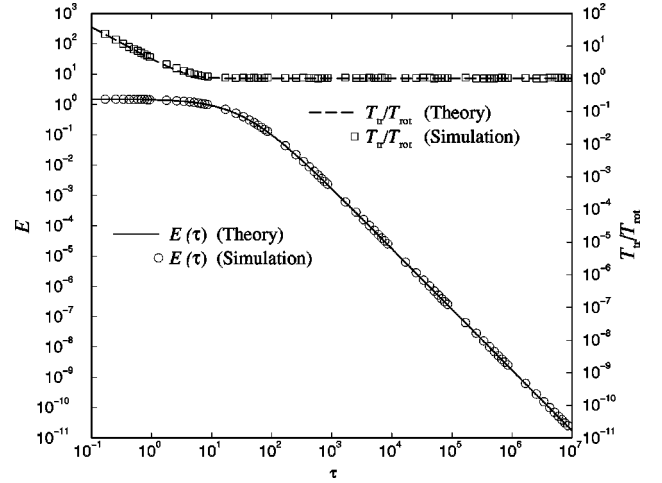

FIG. 2. Double logarithmic plot of total kinetic energy $E=3/2T_{\rm tr}+T_{\rm rot}$ in units of $T_{\rm tr}(\tau=0)$ and of $T_{\rm tr}/T_{\rm rot}$ versus dimensionless time τ. The simulation data are from a system of 10000 needles, box of length 24 L and $\epsilon=0.8$.

Momentum organization of the particles shows up in the hydrodynamic flow field $\rho_\alpha\boldsymbol{U}_\alpha=\langle\boldsymbol{v}_i\rangle_\alpha$. A good indicator [13] for the build up of long range velocity correlations is the ratio of the total kinetic energy of the flow to the total internal energy $S:=[\Sigma_\alpha(m/2)\rho_\alpha\boldsymbol{U}_\alpha^2]/(\Sigma_\alpha\rho_\alpha T_\alpha^{\rm tr})$.

To investigate *orientational ordering* we compute in addition the quadrupolar moment of the needles $Q_i^e:=[3(\boldsymbol{u}_i\cdot\boldsymbol{e})^2-1]$. The unit vector $\boldsymbol{e}$ is chosen either along the direction of the particle's velocity or fixed in space.

VI. SMALL AND MODERATE DENSITIES

For densities such that $(N/V)L^3\lesssim 1$, the system remains homogeneous, orientationally disorderd and without long range velocity correlations up to the longest observed time scales, i.e., when the energy has decayed to 10^{-11} of its initial value. To check for spatial clustering, histograms of fluctuations of the local density, velocity and translational energy were compared to those of an elastic system but no significant difference could be observed. Fluctuations, e.g., of the local density do not increase with time but remain stationary, so that we can compare our approximate theory with the simulations. We show here a simulation which has been performed for 10 000 needles in a box of length 24 L. This corresponds to a density of $(N/V)L^3\approx 0.72$ or an average center of mass separation $l/L\approx 1.1$.

In this range of densities, cooling of a gas of hard needles proceeds in *two stages*. First, there is an exponentially fast decay towards a state which is characterized by a constant ratio of translational and rotational energy. Second, there is an algebraically slow decay of both, the translational and rotational energy, such that their ratio remains constant. Both of these regimes are correctly predicted by our approximate theory, based on the assumption of spatial homogeneity.

In Fig. 2 we plot the numerical solution of Eqs. (14) and (15) for $\epsilon=0.8$ and $k=6$ as a function of dimensionless time $\tau=\gamma\sqrt{T_{\rm tr}(0)}t$. The total kinetic energy $E=\frac{3}{2}T_{\rm tr}+T_{\rm rot}$ [in units of $T_{\rm tr}(\tau=0)$] and the ratio $T_{\rm tr}/T_{\rm rot}$ are compared to simulations. Analytical theory and simulation are found to agree within a few percent over eight orders of magnitude in

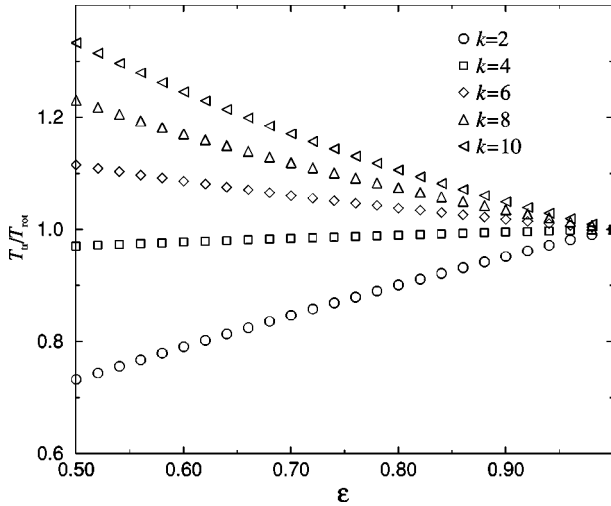FIG. 3. Asymptotic ratio T_{tr}/T_{rot} as a function of ϵ and k.

time. [$T_{rot}(0)=0$ has been chosen as initial condition.]

The decay of T_{tr}/T_{rot} to a constant value happens on a time scale of order one. In this range of times the total kinetic energy E remains approximately constant (on a logarithmic scale) and decays like t^{-2} only *after* translational and rotational energy have reached a constant ratio.

Equations (14) and (15) allow for a solution with a constant ratio of $T_{tr}/T_{rot}=c$ and both T_{tr} and T_{rot} decaying like t^{-2}. To determine the constant c, we plug the ansatz $cT_{rot}=T_{tr}$ into Eqs. (14) and (15) and use $c\dot{T}_{rot}-\dot{T}_{tr}=0$. This yields an implicit equation for c, whose solution is plotted in Fig. 3 as a function of k and ϵ.

Setting $c=1$ in this implicit equation yields an equation for k which reads

$$(1-\epsilon^2)\int_\square d^2r\,\frac{1-\frac{3}{2}k^*r^2}{\sqrt{1+k^*r^2}}=0, \qquad (16)$$

i.e., equipartition holds for *all* values of $\epsilon<1$ if $k=(mL^2)/(2I)$ is set to the particular value $k^*=4.3607$, given as the solution of Eq. (16). For $\epsilon=1$, equipartition always holds, independent of k.

For $k<k^*$ we find $T_{tr}<T_{rot}$ and for $k>k^*$ $T_{tr}>T_{rot}$. Hence the distribution of mass along the rods determines the asymptotic ratio of rotational and translational energy, including equipartition as a special case.

The asymptotic solution discussed above is approached for arbitrary initial conditions for long times. If a totally elastic system is prepared in an initial condition with $T_{tr}\neq T_{rot}$, we expect that the equilibrium state (equipartition) is reached exponentially fast with a relaxation rate given by $\nu\sim\gamma\sqrt{E(0)}$. As long as energy dissipation due to inelastic collisions is small, we expect similar behavior, as indeed the numerical simulations show.

VII. DENSE SYSTEMS

Simulations of inelastic hard spheres show well developed density clusters and vortex patterns [3–5,14], if allowed to evolve freely for sufficiently long times. The domi-
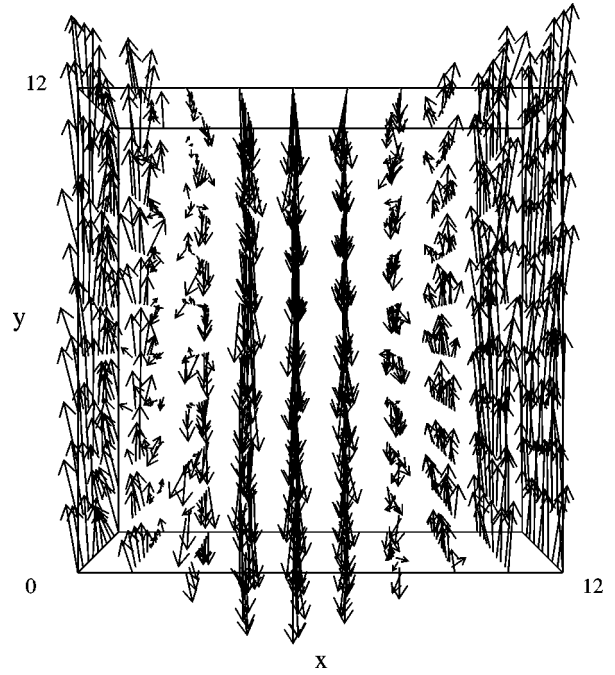

FIG. 4. Flow field of the system [20000 needles in a box of volume $(12L)^3$ and $\epsilon=0.9$] after 600 collisions per particle (the length of the velocity vectors are in arbitrary units).

nant mechanism for the formation of vortex structures has been traced back to noise reduction [15]: After many collisions the particles move more and more parallel. It is not clear *a priori*, whether such a mechanism should also apply to rotating needles. In the simulations we clearly observe the formation of large scale structures in the velocity field. In Fig. 4 we show the hydrdynamic flow field after 600 collisions per particle for a system of density $(N/V)L^3\approx11.6$, corresponding to an average center of mass separation $l/L=0.44$.

We observe two shear bands (note the periodic boundary conditions), which move in opposite directions. Within a band the local flow field is to a large degree aligned. The dominant part of the velocity of each particle $\boldsymbol{v}_i$ is given by the flow U so that a large fraction of the kinetic energy is in the flow and the ratio S (defined in Sec. V) should be high. In Fig. 5(a) we show S as a function of the number of collisions per particle. S increases from a value of 0.05 to a value of about 2.5, i.e., by a factor of 50.

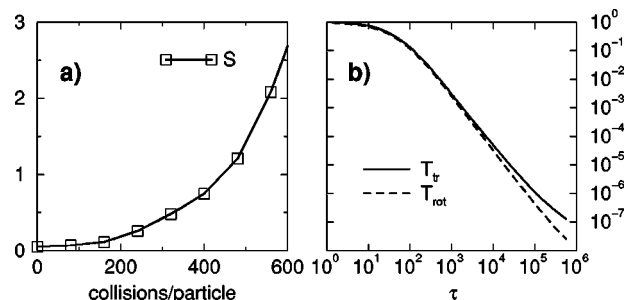To visualize spatial inhomogeneities we plot in Fig. 6

FIG. 5. (a) S as a function of collisions per particle. (b) Double logarithmic plot of kinetic energy per degree of freedom T_{tr} and T_{rot} in units of $T_{tr}(\tau=0)$ versus dimensionless time τ.
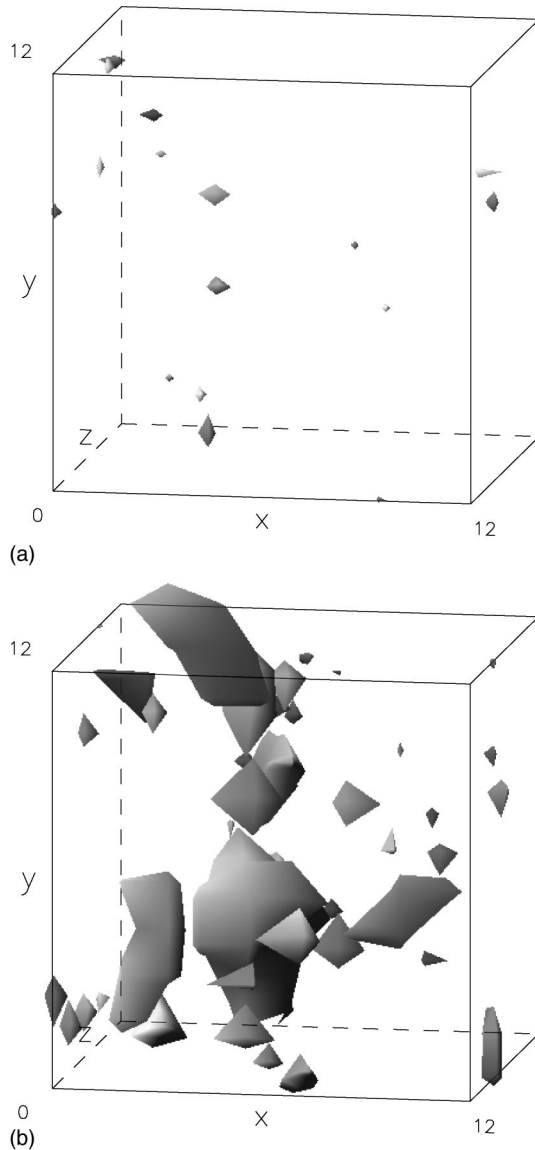
(a)

(b)

FIG. 6. (a) Density at the beginning of the simulations. Only very few and small regions have a more than 50 % higher density than average. (b) Large regions with higher density have built up after 600 collisions per particle.

regions with local deviation of the density $\Delta\rho_\alpha > 0.5$ at the beginning of the simulation and after 600 collisions per particle. Obviously clustering occurs. To quantify this observation we have computed the second moment of the density fluctuations. It is found to increase by a factor of 6 over its initial value after 400 collisions. After about 500 collisions per particle it decreases again, indicating that clusters form and dissolve again.

For spheres one observes [3,4,14] that most of the mass is concentrated in the two counterflowing streams. To check for correlations between flow field and mass density, we plot in Fig. 7 the components of the flow field U_y, U_z and the density fluctuation as a function of x, for fixed $y = 6L$ and averaged over 10 values of $z = 1.2L, \ldots, 12L$. This and similar plots give no hint of a strong correlation between flow field and density fluctuations.

We also observe a weak tendency towards organization of rotational velocities. The ratio of the kinetic energy of the
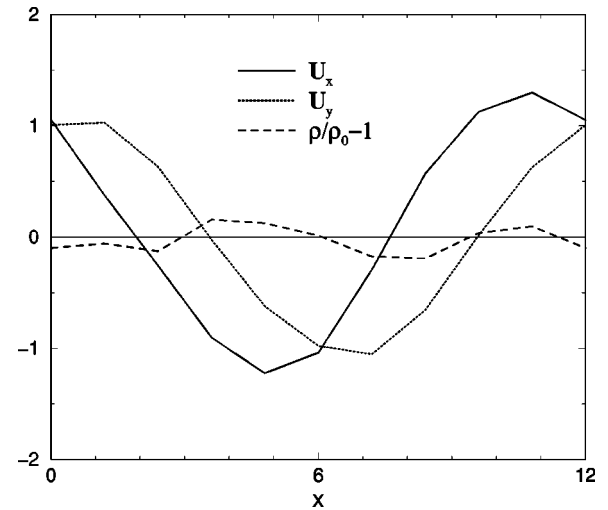

FIG. 7. y and z component of the flow field and fluctuation of the density as a function of x, for fixed $y = 6L$, averaged over 10 z values.

local rotational flow to the local rotational temperature is found to increase by about 50% (as compared to an increase by a factor of 50 for the translational velocity). Consequently, the deviation from Haff's t^{-2} cooling law is much stronger for the translational degrees of freedom T_{tr} than for the rotational degrees of freedom T_{rot} [see Fig. 5(b)].

To investigate alignment of the needles with the large scale velocity flow field, we compute the quadrupolar momentum Q_i^e with respect to the particle velocity, i.e., $e = v_i/|v_i|$. A histogram over all needles is shown in Fig. 8. The configuration after 600 collisions per particle is compared to the initial state which corresponds to randomized orientations. In addition we plot the theoretical prediction for the histogram (straight line) which has been calculated on the assumption that rods are oriented randomly and independent of their velocity. No indication for alignment of the needles can be seen. Neither do we observe a tendency for global ordering.
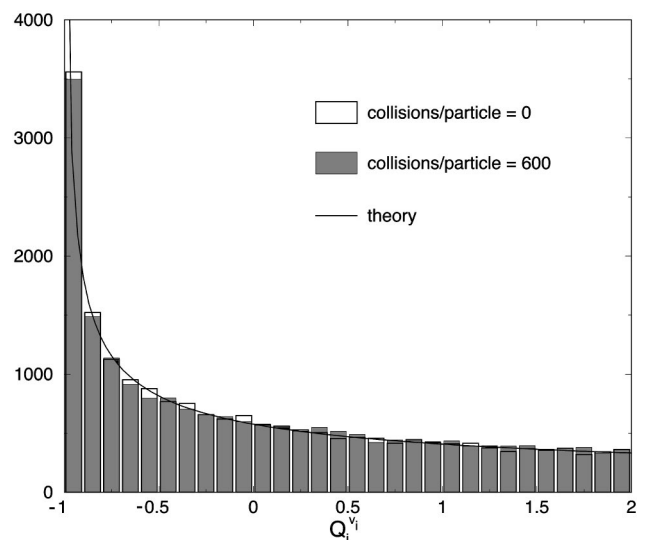

FIG. 8. Histogram of Q_i^e. The distribution after 600 collisions per particle coincides with the initial distribution and with the prediction for randomly distributed orientations.

VIII. CONCLUSION AND OUTLOOK

Our aim was to systematically investigate the cooling dynamics of a granular system of nonspherical objects. We have chosen the simplest nonspherical grains, hard needles, for which we were able to formulate an approximate kinetic theory, generalizing methods of kinetic theory of elastic systems [7] to inelastic collisions with normal and tangential restitution. In addition, simulations of large systems for various densities have been performed.

Analytical theory is so far restricted to the regime of moderate densities, where the interparticle spacing is comparable to or larger than the length of the needles. Such systems remain homogeneous and show no long range correlations in the velocity field or orientation. Cooling proceeds in two stages: (1) An exponentially fast initial decay towards a state with constant ratio of translational to rotational energy and (2) an algebraically slow decay, such that the above ratio remains constant in time. The ratio of translational to rotational energy is controlled by the coefficient of normal restitution and by the distribution of mass along the rods.

Simulations in the dense regime, where the interparticle spacing is smaller than the length of the needles, reveal large scale structures in the translational velocity field. The density does not remain homogeneous, but clusters form and dissolve again. Cooling proceeds in three stages. For short and intermediate time scales the relaxation is similar to the low density system, whereas on the longest time scales we observe a crossover from the algebraic decay to an even slower decay. This latter decay may be identical to the asymptotic cooling law of hard inelastic spheres, $\tau^{-d/2}$ in d dimensions, where τ is the average number of collisions suffered by a particle within time t, which has been derived in [13].

We plan to generalize the hydrodynamic analysis to grains with rotational degrees of freedom and in particular hard rods. Another possible extension of our work are rods of finite width and with spherical endcaps.

[1] For an overview see, e.g., *Physics of Dry Granular Media*, Vol. 350 of *NATO Advanced Study Institute, Series E: Applied Science*, edited by H. J. Herrmann, J.-P. Hovi, and S. Luding (Kluwer Academic Publishers, Dordrecht, The Netherlands, 1998).

[2] J. T. Jenkins and M. W. Richman, Phys. Fluids **28**, 3485 (1985); C. K. K. Lun and S. B. Savage, J. Appl. Mech. **54**, 47 (1987); C. K. K. Lun, J. Fluid Mech. **233**, 539 (1991); A. Goldshtein and M. Shapiro, *ibid.* **282**, 75 (1995).

[3] I. Goldhirsch and G. Zanetti, Phys. Rev. Lett. **70**, 1619 (1993).

[4] S. McNamara and W. R. Young, Phys. Rev. E **53**, 5089 (1996).

[5] T. P. C. van Noije, M. H. Ernst, R. Brito, and J. A. G. Orza, Phys. Rev. Lett. **79**, 411 (1997).

[6] T. P. C. van Noije and M. H. Ernst, Physica A **251**, 266 (1998).

[7] D. Frenkel andj J. F. Maguire, Mol. Phys. **49**, 503 (1983).

[8] B. Cichocki, Z. Phys. B **66**, 537 (1987).

[9] M. H. Ernst, J. R. Dorfmann, W. R. Hoegy, and J. M. J. van Leeuwen, Physica (Amsterdam) **45**, 127 (1969).

[10] M. Huthmann and A. Zippelius, Phys. Rev. E **56**, R6275 (1997).

[11] B. D. Lubachevsky, J. Comput. Phys. **94**, 255 (1991).

[12] S. Luding and S. McNamara, Granular Matter **1**, 113 (1998).

[13] R. Brito and M. H. Ernst, Europhys. Lett. **43**, 497 (1998).

[14] I. Goldhirsch, M. L. Tan, and G. Zanetti, J. Sci. Comput. **8**, 1619 (1993).

[15] R. Brito and M. H. Ernst, Int. J. Mod. Phys. C **9**, 1339 (1998).